Available online at www.sciencedirect.com
ScienceDirect
International Journal of Mass Spectrometry 263 (2007) 204–212
International Journal of Mass Spectrometry
www.elsevier.com/locate/ijms

Collision induced dissociation study of 10 monoterpenes for identification in trace gas measurements using the newly developed proton-transfer reaction ion trap mass spectrometer

M.M.L. Steeghs *, E. Crespo, F.J.M. Harren

Life Science Trace Gas Facility, Molecular and Laser Physics, Institute for Molecules and Materials, Radboud University, P.O. Box 9010, NL-6500 GL Nijmegen, The Netherlands

Received 2 October 2006; accepted 9 February 2007
Available online 15 February 2007

Abstract

We present the study of fragmentation patterns of different monoterpene species after dissociative proton-transfer and after collision induced dissociation (CID) in a newly developed proton-transfer reaction ion trap mass spectrometer (PIT-MS). For the monoterpene measurements the proton-transfer reaction chamber was set at an *E*/*N*-value of 90–100 Td; at this value the monoterpenes can be found at *m*/*z* values of 137 and 81. CID patterns of all 10 monoterpenes studied are found to be distinguishable, making it possible to positively identify a monoterpene solely on the basis of its CID pattern. However, identification of compounds in a mixture of several monoterpenes will still be difficult. Additionally, we find that the outcome of a CID experiment, expressed in the ratio between different fragments, depends on the kinetic energy of the ions as they exit the drift tube. This behavior is attributed to differences in ion internal energy at different drift tube voltages. The effect of ion internal energy change on the CID pattern is shown when the cooling time between isolation and dissociation of the parent ions is changed, and the CID fragmentation ratio of fragments 95 and 81 amu of α-terpinene is affected.

Keywords: PTR-MS; PIT-MS; Ion trap; Volatile organic compound; Trace gas detection

1. Introduction

Proton-transfer reaction mass spectrometry (PTR-MS) has proven itself over the last decade as a versatile, sensitive, online monitoring technique for a large variety of volatile organic trace gas compounds [1]. Its high sensitivity, the fact that there is no need for sample preconcentration, its high temporal resolution, relatively low degree of fragmentation due to low excess energy of the proton-transfer reaction and the fact that it cannot measure the normal constituents of air (e.g., O_2, NO, NO_2, CO, CO_2), make it an excellent technique to monitor trace gas compounds in real-time. Numerous examples of application of the PTR-MS technique in various fields including atmospheric science [2–4], post-harvest research [5,6], medical diagnostics [7–10], plant biology [11–14], food technology [15–17] and industrial process [18,19] monitoring have appeared in literature since its first appearance in the mid 1990s. These widely varied applications show the strength and diversity of the PTR-MS technique. Its limitations, however, have also been shown in several publications (cf. [11,20–22]). Since PTR-MS instruments are historically equipped with a quadrupole mass filter, it will generally not be possible to positively identify the compounds emitted by the object under study. When the mass of an observed compound increases, also the amount of possible identities for the characteristic ion and parent neutral compound increases. Several solutions have been proposed to tackle this problem, including the coupling of a gas chromatograph to the PTR-MS or the serial or parallel use of GC–MS. The major drawback of this approach is that the online monitoring capability of the PTR-MS is lost.

A promising new development is the use of an ion trap mass spectrometer (IT-MS) instead of a quadrupole mass filter. A few

* Corresponding author. Tel.: +31 24 3652171; fax: +31 24 3653311.
E-mail address: m.steeghs@science.ru.nl (M.M.L. Steeghs).

1387-3806/$ – see front matter © 2007 Elsevier B.V. All rights reserved.
doi:10.1016/j.ijms.2007.02.011

different groups have now developed such a PIT-MS system and have shown it is a reliable and highly interesting improvement on the PTR-MS techniques [21,23–26]. Most of the advantages of an IT-MS over a quadrupole mass filter have been discussed in detail before [21,22,25,26] and include the higher duty cycle, the possibility to perform ion–molecule reactions inside the trap, the ability to work with higher drift tube pressures and the possibility to perform collision induced dissociation (CID) in the trap. The increased drift tube pressure has the advantage of increased sensitivity [25] and of decreased fragmentation following proton-transfer [26]. Especially the CID approach is a promising tool that can become a very useful, routinely applied method to characterize the volatile mixture under analysis, maintaining the online capabilities of the continuous flow drift tube technique. The applicability of CID to the identification of atmospherically interesting compounds [21] and in the analysis of the C_6-aldehydes emitted from drying rice and sorghum [24] has recently been shown. Also some volatiles emitted by an apple have been successfully studied using CID [26].

Another group of VOCs that is potentially very interesting to investigate with PIT-MS is constituted by the monoterpenes. Terpenes and their oxygenated derivatives are emitted from many products such as fruits and natural aromas [27]. They are also important in atmospheric chemistry and many plants, especially pine trees, are known to emit monoterpenes [28,29].

In this publication, we investigate the CID patterns of 10 monoterpenes using our newly developed PIT-MS instrument. These monoterpenes are generally observed at the same mass (137 amu, with a main fragment on mass 81 amu and sometimes additional minor fragments [27,30]) and the signal on this mass is usually referred to as the sum of all monoterpenes emitted [30,31]. Since there are many different monoterpenes that can be measured, it is a challenge for PIT-MS to identify individual compounds from their CID patterns. Additionally, the stability of the CID patterns under different drift tube conditions and the influence of helium pressure and resonant excitation stability parameters on the CID patterns and the eventual fragment ratios are presented. The effect of a cooling period between isolation and dissociation is investigated.

2. Materials and methods

2.1. The proton-transfer reaction ion trap mass spectrometer (PIT-MS)

The PIT-MS instrument used in this study (Fig. 1) is based on a commercially available PolarisQ GC–IT–MS system (Thermo Finnigan PolarisQ, Interscience, Breda, the Netherlands), adapted for use with a proton-transfer reaction cell. The instrument has been described in detail by Steeghs et al. [26]. It principally is an advanced version of the proton-transfer reaction mass spectrometer (PTR-MS) systems that have found ample use in trace gas detection over the last decade. In short, the PIT-MS technique is as follows: neutral molecules to be detected are

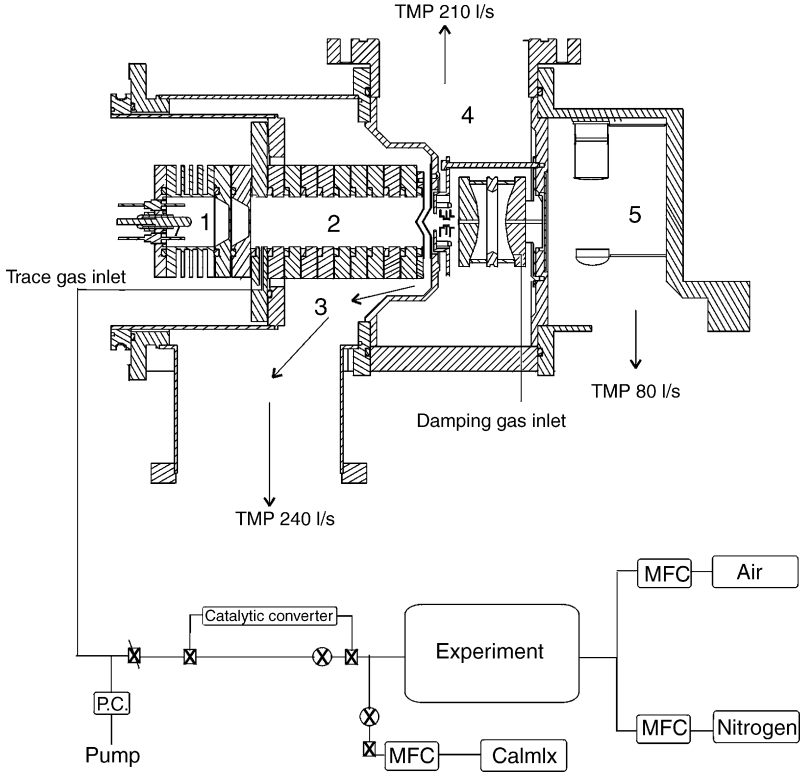

Fig. 1. Schematic view of the proton-transfer reaction ion trap mass spectrometer (PIT-MS) with inlet system. The PIT-MS system consists of (1) an ion source for the production of H_3O^+-ions, (2) a drift tube, in which the proton-transfer reaction takes place, (3) a transition chamber that pumps the drift tube and provides a proper pressure for, (4) the ion trap chamber in which the ion trap mass spectrometer and a set of focusing/gating lenses are located and where the helium damping gas is led directly into the trap (5) the detector chamber containing a conversion dynode and a channeltron secondary electron multiplier used in analog current detection mode.

ionized in a drift tube via a proton-transfer reaction with H_3O^+:

$$H_3O^+ + R \xrightarrow{k} RH^+ + H_2O$$

where k is the reaction rate constant, usually close to or equal to the collision rate constant. This reaction only takes place when the proton affinity (PA) of the trace compound R is higher than that of water (166.5 kcal/mol = 7.16 eV). A major advantage of using H_3O^+ as the reagent ion is that the PA of water is higher that the PA of the normal constituents of air (cf. NO, O_2, CO, CO_2, and N_2) and that most of the typical organic compounds are ionized by the proton-transfer (PT) reaction, since their PA are in the range between 7 and 9 eV. Since the excess energy of the reaction is low, fragmentation only occurs to a very limited degree, resulting in only one or two characteristic ions per VOC.

The ions formed in the drift tube are extracted towards an ion trap mass spectrometer, where they are accumulated and mass analyzed and subsequently detected by a conversion dynode/electron multiplier assembly. The ion trap mass spectrometer consists of a central ring electrode with an inner radius $r_0 = 7.07$ mm, driven with an rf frequency of 1.02 MHz, and two end caps with $z_0 = 7.85$ mm (z_0 is half the distance between the two end caps) with an opening of ~1.1 mm on each end. The electrodes are isolated by ceramic rings in a closed setup. The helium damping gas (>99.999% purity) is added through a hole in the side of the exit end-cap electrode. Ions are focused into the ion trap by a set of three electrostatic lenses of which the second is a gate lens to allow the ions into the trap. Filtered noise fields (FNF) are applied to the end-caps to resonantly eject specific m/z values from the trap or to resonantly excite pre-selected m/z values for collision induced dissociation analysis. No automatic gain control is used. All mass spectrometer actions are controlled by an adapted "Custom Tune" module accompanying the standard PolarisQ control software "Excalibur".

2.2. Measurements

Monoterpenes can be seen as a combination of two isoprene entities C_5H_8 and may be saturated, unsaturated, cyclic or acyclic. Their different isomers may differ only by as much as the position of a double bond. The CID-patterns of 10 different monoterpenes (pure compounds; Sigma–Aldrich Chemie BV, Zwijndrecht, the Netherlands) are measured, of which only one (myrcene) is acyclic (Fig. 2).

A few milliliter of pure compound is put into a small septum-capped vile. A needle through the septum provides a diffusion path from the small vile into a 1 l cuvette. The headspace of this big cuvette is flushed with nitrogen and analyzed by the PIT-MS. For all 10 monoterpenes, the CID-patterns of the most prominent fragments (including the parent ion) are made and the fragmentation ratios due to dissociative proton-transfer reactions as a function of E/N-value (E/N, drift tube electric field divided by the gas number density, a measure of the kinetic energy of ions in the drift tube, expressed in Townsend; 1 Td = 10^{-17} V cm^2) are determined for 8 monoterpenes.

CID patterns are plot as the relative ion intensity as a function of resonant excitation energy. At each value for the resonant excitation energy, 10 mass scans of the CID products (+parent ion) are made and averaged. The fragment values are determined as follows:

$$I_{\text{norm}} = \frac{I}{P_0}$$

$$I_{\text{rel}} = \frac{I_{\text{norm}}}{\sum_i I_{\text{norm},i}}$$

where I_{norm} is the normalized ion intensity, I the measured intensity of the ion (fragment ions as well as parent ions) and P_0 is the intensity of the parent ion at zero excitation amplitude. I_{rel} is the value for the intensity, expressed as a fraction of the sum of all (normalized) ion signals. The ratio between fragments is determined as the average of the last three or four energies of the CID pattern. These fragmentation ratios, and sometimes the dissociation threshold, are the values that can be compared for different compounds.

The influences of buffer gas pressure and stability parameter during resonant excitation are investigated by comparing the CID pattern of acetone at different values of these parameters.

The effect of changing drift voltage values is monitored by measuring the CID patterns of 5 different monoterpenes at E/N-values ranging from 80 to 140 Td.

To check if the ion internal energy is affecting the CID pattern, the cooling time between isolation and dissociation is varied and the ratio between fragment masses 95 and 81 amu of α-terpinene are monitored.

3. Results

3.1. Fragmentation patterns upon proton-transfer

Fig. 3 shows the fragment ratios of 8 monoterpenes as a function of E/N-value for the dissociative proton-transfer reaction. All 8 monoterpenes have major fragments on only masses 81

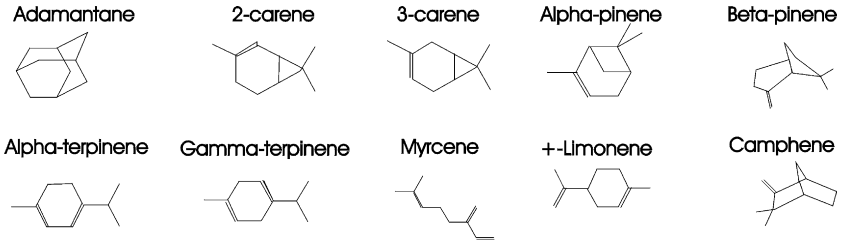

Fig. 2. The structures of the monoterpenes used in this study.

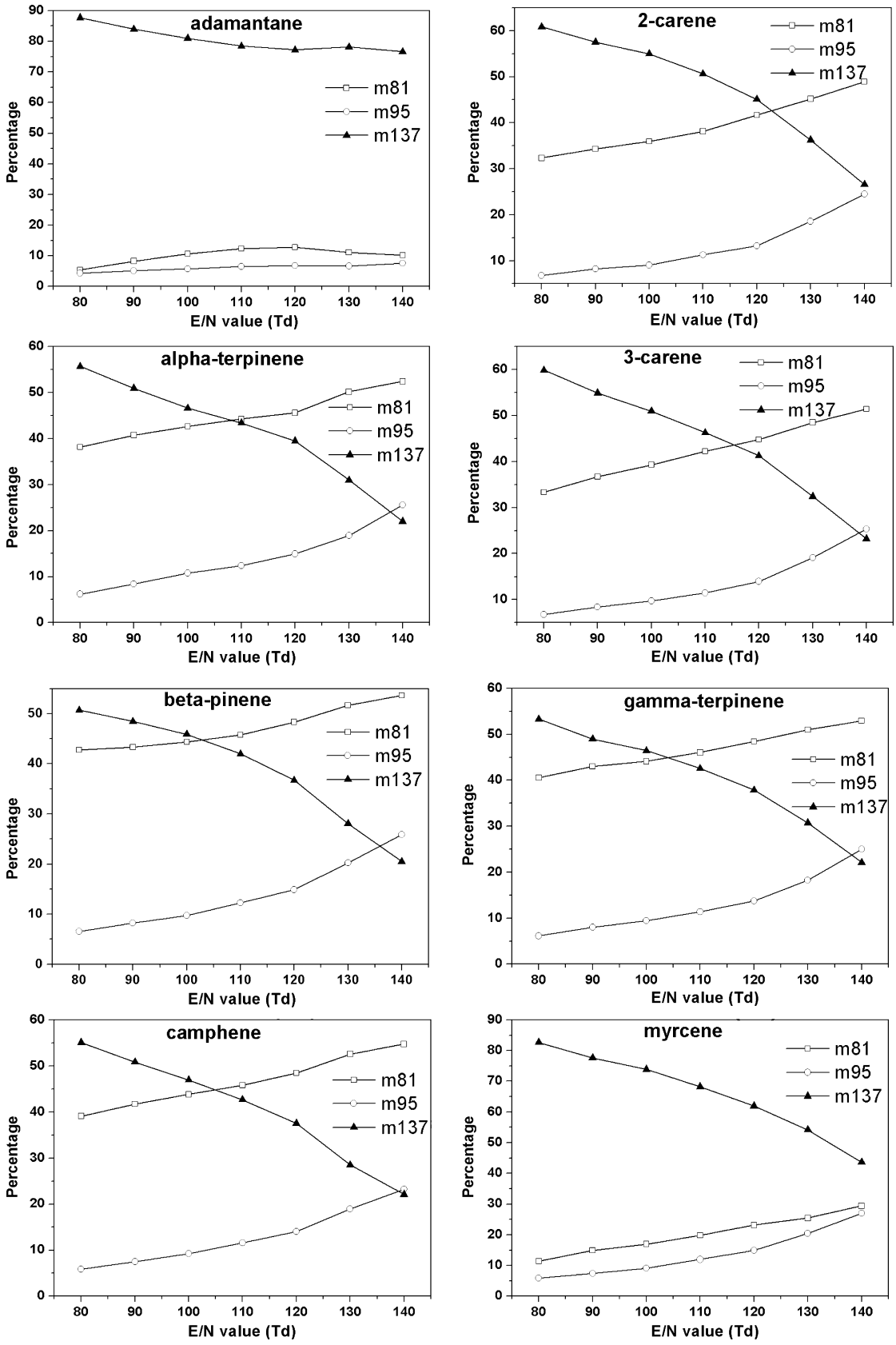

Fig. 3. Fragmentation patterns as a function of *E*/*N*-value in the drift tube of the monoterpene species adamantane, α-pinene, β-pinene, camphene, 2-carene, 3-carene, γ-terpinene and myrcene.

Table 1
Fragmentation ratios due to dissociative proton-transfer from H_3O^+ to the monoterpenes investigated in this study at 100 Td and at 120 Td

Compound	100 Td			120 Td		
	m137 (amu (%))	m95 (amu (%))	m81 (amu (%))	m137 (%)	m95 (%)	m81 (%)
Adamantane	81	6	11	77	7	13
β-Pinene	46	10	44	37	15	48
2-Carene	55	10	36	45	13	42
3-Carene	51	10	39	41	14	45
α-Terpinene	47	11	43	40	15	46
γ-Terpinene	46	10	44	38	14	48
Camphene	47	9	44	38	14	48
Myrcene	74	10	17	62	15	23

The sum of the fractions is set to 100%. For some, an additional small fragment (<5%) is observed but not given in the table, so the sum of m137, m95 and m81 might not add up to 100%.

($C_6H_9^+$) and 95 amu ($C_7H_{11}^+$), where 81 amu almost always is the dominant fragment mass. Only in the case of myrcene and adamantane, the fragment on 95 is of comparable intensity as the fragment on mass 81 amu. Adamantane hardly fragments at all, and for myrcene only at higher *E*/*N*-values fragmentation becomes important. Every other compound has some other minor fragments (<2%, e.g., mass 107 for adamantane <5% at 140 Td and <2% at 100 Td), but those will not be observable or quantifiable in biological samples and are therefore ignored. The fragmentation ratios from the dissociative proton-transfer reactions for the different monoterpenes, as obtained with our PIT-MS system are given in Table 1.

In recent work [26], we showed that the PIT-MS can handle cluster ions much better than a PTR-MS can, as a consequence of which the *E*/*N*-value in the drift tube can be reduced considerably. An optimal *E*/*N*-value of ~95 Td was found for most of the compounds explored. Fig. 4 shows the absolute (normalized) ion intensity of the sum of the fragments and of the parent ion mass 137 amu as a function of *E*/*N*. This graph only gives information about the relative sensitivity per monoterpene as a function of *E*/*N*-value, since the concentration of the monoterpenes is constant over the whole experiment, but unknown. From Fig. 4, we find again an optimal sensitivity between 90 and 100 Td.

3.2. Collision induced dissociation

At 100 Td, for all the monoterpenes, mass 137 amu is the dominant mass. Fig. 5 shows the CID patterns of mass 137 of the monoterpenes myrcene, adamantane, 2-carene and 3-carene. This figure clearly shows the differences that can be found between the CID patterns of the various monoterpenes. We can distinguish between 2-carene and 3-carene by the difference in m95/m81 ratio, while myrcene shows a small but significant fragment on mass 107. Adamantane shows a completely different CID pattern, where the two dominant fragments are mass 107 and 93, with a smaller fragment on mass 79.

For all the monoterpenes studied here, the CID patterns of the "proton-transfer fragments" 95 amu and 81 amu are identical. Fig. 6 displays the CID patterns of masses 95 amu and 81 amu of adamantane as an example for these patterns. To identify various monoterpenes by their CID pattern, we could use both the (relative) dissociation threshold (the lowest resonant excitation waveform amplitude at which the major CID fragment is detected) and the final ratio between different fragments. As will be shown below, the dissociation threshold depends strongly on instrumental parameters. Therefore, to be able to compare different PIT-MS instruments in the future, the final ratio between the different fragments or a list of the fraction of the CID prod-

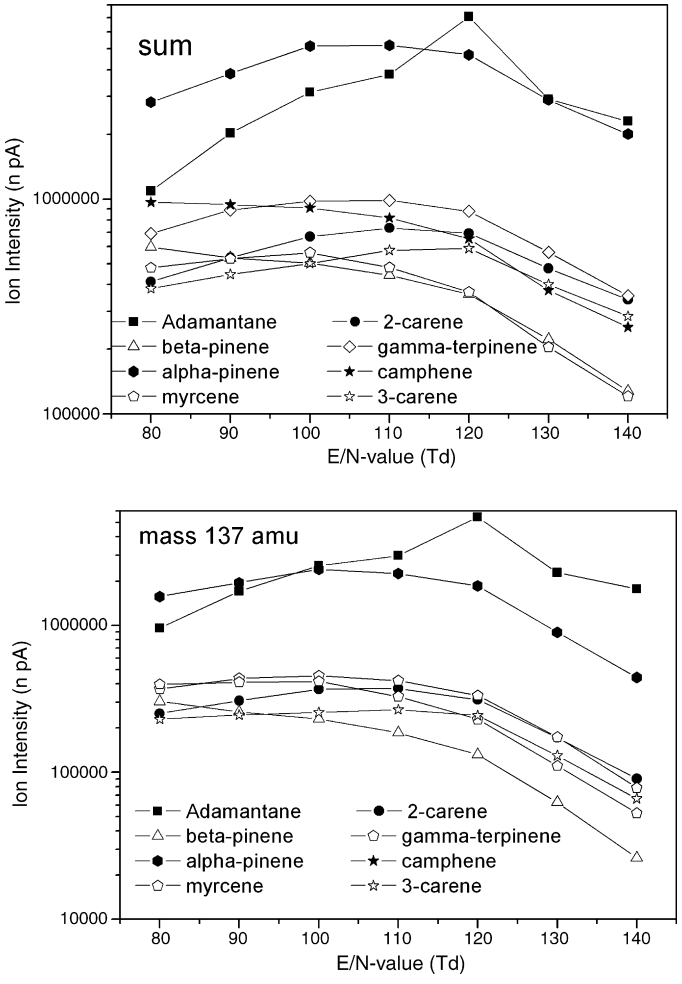

Fig. 4. The sum of ion intensities of the major fragments (top panel) and of mass 137 (bottom panel) is shown as a function of *E*/*N*-value in the drift tube for 8 different monoterpenes.

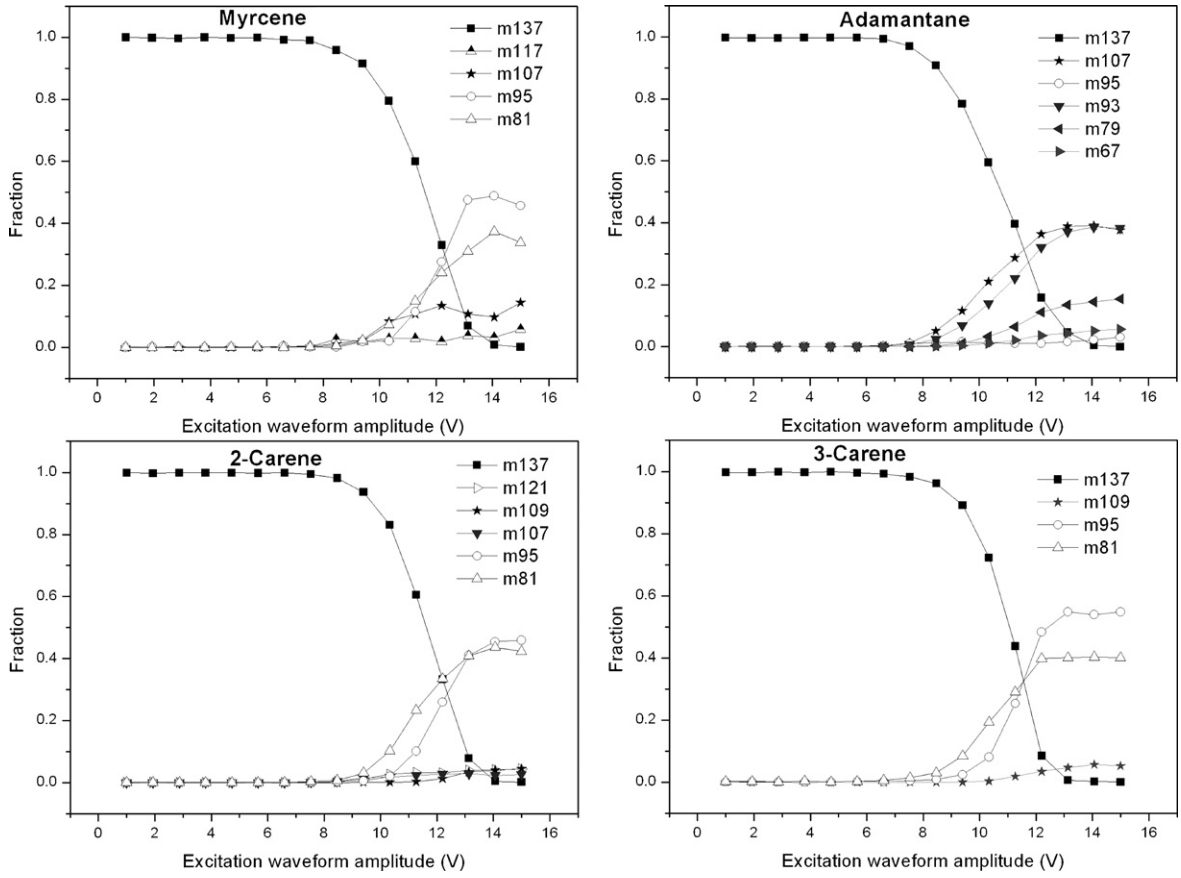

Fig. 5. CID patterns of the parent ion of myrcene, adamantane, 2-carene and 3-carene in the ion trap. Fragmentation fractions are shown as a function of the excitation waveform amplitude in the trap.

ucts is used. Table 2 gives these values for all 10 monoterpenes investigated in this work.

3.3. Influence of system parameters on CID patterns

Three of the parameters that influence the CID behavior are investigated: the helium pressure in the ion trap, the resonant excitation q_z stability parameter and the *E*/*N*-value in the drift tube. Here, we use acetone as an example. The helium pressure in the ion trap is important, since it has two effects. On one hand, the helium scavenges kinetic energy from the ions in the trap by elastic collisions. On the other hand, when the kinetic energy of a stored ion is increased far enough, inelastic collisions with the helium buffer gas can cause collision induced dissociation.

Fig. 7 shows the influence of the helium pressure on the dissociation pattern. As shown for acetone the dissociation threshold shifts to higher voltages at increased helium pressures, showing the increased damping effect. Also displayed is the final m41/m31 fragment ratio, which is not affected by increased helium pressure. The point at 16% damping gas flow (optimal trap performance is found around 11% helium flow, corresponding to $p \sim 1 \times 10^{-3}$ mbar) is increased due to the shifted dissociation threshold value. The maximum fluence (product of excitation waveform amplitude and duration) applied could not

Table 2
Final CID fragment ratios of 10 monoterpenes

Compound	Highest fragment (amu (%))	Second mass (amu (%))	Third mass (amu (%))	Fourth mass (amu (%))	Fifth mass (amu (%))	Ratio m95/m81
Adamantane	107 (38)	93 (36)	79 (14)	67 (5)	95 (2)	n.a.
α-Pinene	95 (54)	81 (34)	117 (12)			1.588
β-Pinene	95 (49)	81 (44)	109 (5)	121 (2)		1.114
2-Carene	95 (44)	81 (42)	121 (4)	109 (4)	107 (3)	1.048
3-Carene	95 (53)	81 (40)	109 (5)			1.325
α-Terpinene	95 (46)	81 (41)	109 (4)	121 (2)		1.122
γ-Terpinene	95 (48)	81 (39)	109 (4)	107 (3)	121 (3)	1.23
Camphene	95 (49)	81 (39)	107 (4)	109 (4)		1.256
Myrcene	95 (47)	81 (36)	107 (12)	117 (5)		1.306
(+)-Limonene	95 (49)	81 (39)	107 (7)	121 (4)		1.256

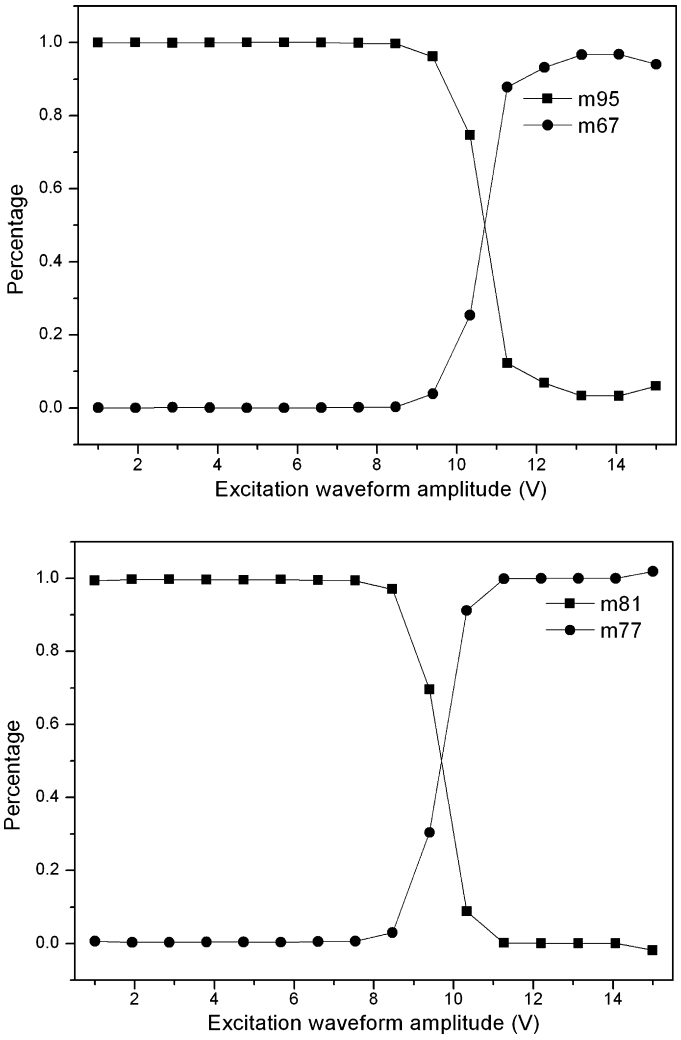

Fig. 6. CID patterns of the two major proton-transfer fragments of adamantane are shown as a typical example for further dissociation of fragments in the ion trap. Fragmentation fractions are shown as a function of the excitation waveform amplitude in the trap.

fully dissociate the trapped ions. This is reflected by the large error bar.

It is known that the CID results in terms of efficiency depend on the resonant excitation q-value (q_z-stability parameter, given by $q_z = 8\,\mathrm{eV}/(m(r_0^2 + z_0^2)\Omega^2)$, corresponding to a set amplitude of the drive frequency Ω) [32,33]. The working point at which CID is performed strongly influences the trapping efficiency of the dissociation products (see Fig. 8). The trapping efficiency is defined as the ratio between the number of fragment ions stored and the number of ions stored before dissociation. The loss is determined by the ion motion pathways that exceed the physical boundaries of the trap. Both trapping and dissociating effects are induced by the excitation waveform. The optimal q_z-value for dissociation efficiency that is used in all experiments was 0.325, which is used in all experiments. Again, when the fragmentation product intensities are expressed as fractions of the total ion intensity left after dissociation, the fractions are constant and the ratios are not affected by the q_z parameter over a large width of q_z-values.

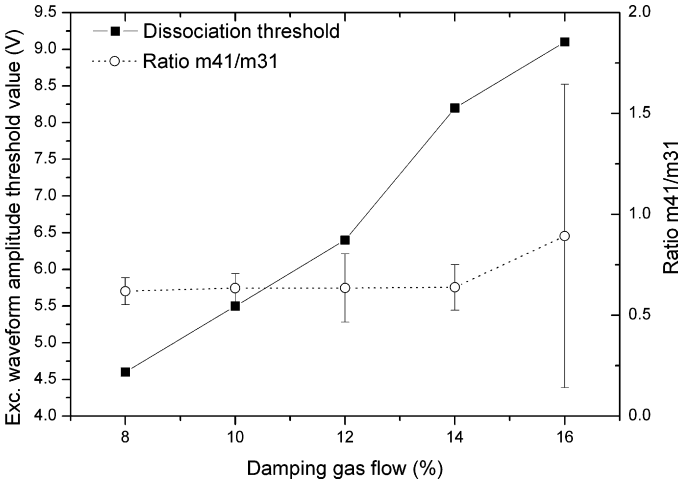

Fig. 7. Influence of the He damping gas flow in the ion trap on the dissociation threshold and fragment ratio for acetone. Here, the dissociation threshold is determined as the minimally needed amplitude for the excitation waveform to observe mass 31 amu as a fragment. The dissociation threshold increases due to the increased He damping effect. The fragmentation ratio is independent on the He flow (and subsequent pressure in the trap): the mass 41/31 ratio is constant. Due to the high dissociation threshold the 16% helium flow value has a large uncertainty.

Fig. 9 shows the dependency on the E/N-value in the drift tube of the m95/m81 CID fragment ratio for 5 different monoterpenes. The fragment at mass 81 decreases with increasing E/N-value, which results in an increasing m95/m81 ratio. To investigate if the decrease of fragment m81 is caused by the high internal ion energy, the effect of a variable 'cooling time' on the CID pattern is measured. The cooling time is the time between finalizing the isolation of the ion to be fragmented and the starting of the CID; the rf voltage amplitude is maintained constant and the ions are not subjected to dissociation yet. Such

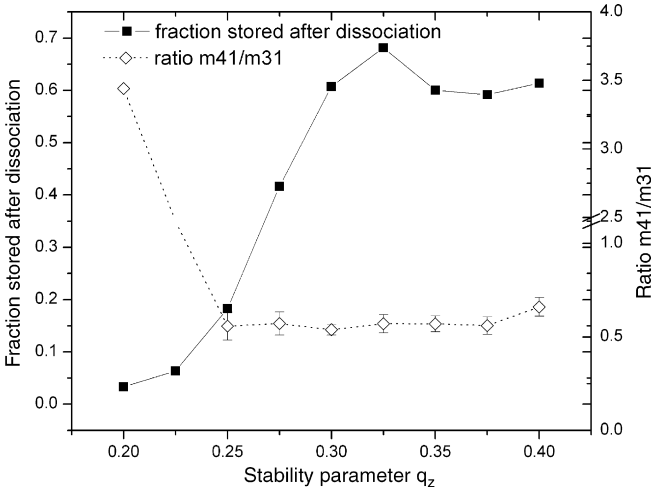

Fig. 8. Influence of the stability parameter q_z on the storage efficiency in the trap and the fragmentation ratio for acetone. The storage efficiency is calculated as the number of ions stored at maximum excitation waveform amplitude, relative to the number of ions stored at zero amplitude voltage. An optimum value is found at $q_z = 0.325$. The fragmentation mass 41/31 ratio is found to be relatively independent for the q_z-value showing that a sufficient fraction of the initial ions is still stored after dissociation.

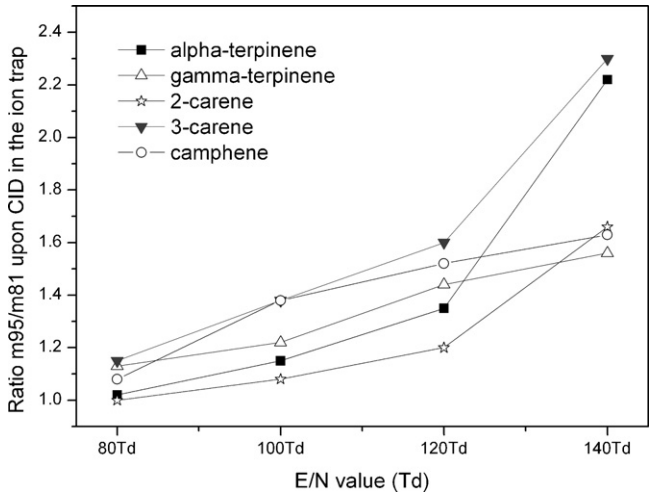

Fig. 9. Influence of the *E*/*N*-value in the drift tube on the fragmentation ratio between fragment ions at *m*/*z* 95 and 81 amu following CID in the ion trap.

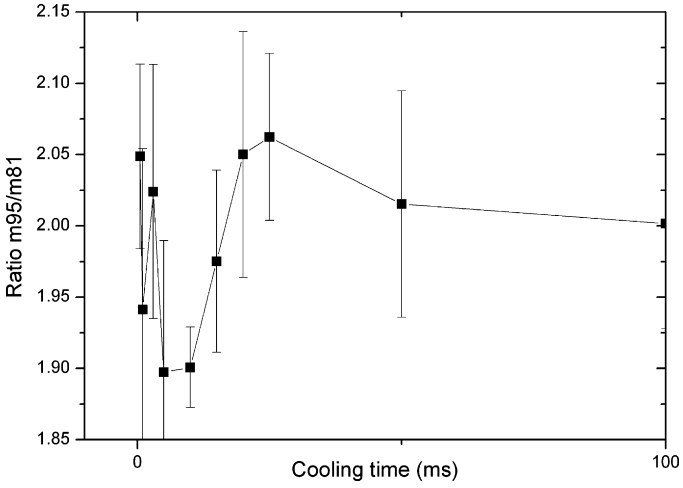

Fig. 10. Effect of a cooling period between isolation and excitation of the trapped ions in the ion trap on the ratio between the two fragments produced upon CID. Clear internal energy dependence is observed.

a delay permits collisional relaxation of the internal energy via collisions with the helium. Fig. 10 shows the effect of such a cooling time on the ratio between fragments m95 and m81 of α-terpinene at 140 Td, which closely resembles an experiment performed by Liere et al. [33] using *n*-butylbenzene.

4. Discussion and conclusion

Here we investigated the fragmentation patterns of the dissociative proton-transfer reaction of H_3O^+ with 8 different monoterpenes and the collision induced dissociation patterns of 10 different monoterpenes with our newly developed PIT-MS instrument. Additionally we studied the influence of 3 important instrumental parameters on the outcome of the CID experiments in order to find out how universal the obtained CID results are. We show that the PIT-MS technique forms a very useful addition to conventional PTR-MS by offering means of identification of different isomeric compounds.

Dissociative proton-transfer reactions of H_3O^+ with various monoterpenes have been studied by Wang et al. in a selected ion flow tube mass spectrometer (SIFT-MS) [27]. They reported only a major fragment on mass 81 amu, with most of the ion intensity found on mass 137 amu. They found that only two monoterpenes (the two limonene compounds) show a very limited degree of fragmentation (3%) on mass 95. Schoon et al. [34] also used SIFT-MS to study the reactions with monoterpenes and they report very limited <8% fragments on either mass 93 or mass 95 amu. This difference in fragmentation patterns as compared to our study can be explained by realizing that the kinetic energy in a drift tube is much higher than in a flow tube as t employed in a SIFT-MS, leading to increased dissociation upon proton-transfer. Several studies published measuring monoterpenes with PTR-MS. Mainly, monoterpenes are monitored on mass 137 amu with the major fragment on mass 81 amu and only fragments of a few percent on mass 93 or 95 [3,27,30,34–36]. Here we find, next to a fragment on mass 81, significant fragmentation on mass 95, not on mass 93. Additionally, fragmentation occurs to a higher degree than found in most PTR-MS systems. Possibly this occurs due to dissociation upon trapping or isolating in the ion trap. It has been shown that the internal energy of trapped ions increases during the isolation process, when the ion trap drive voltage is ramped to the isolation *q*-value [33,37]. A second cause could be an increase in kinetic energy in the buffer chamber of our PIT-MS instrument.

We report the first dissociation patterns on 10 monoterpenes in an attempt to distinguish between different monoterpenes based on their CID patterns. All 10 monoterpenes have distinctive features in their CID pattern. In some cases it is the ratio between mass 95 and 81 amu that distinguishes them from the others. In other cases, it is a unique fragment, or the combination of both. Adamantane shows a completely different CID behavior. It will be possible to identify a single monoterpene solely on the basis of these differences. Of course, when a mixture of multiple monoterpenes is monitored, identification gets more complicated and it depends on the relative amounts and the identity of the monoterpenes in the mixture whether it is possible to identify all products and determine their mixing ratios. Additionally, we realize that there exist more monoterpenes than the 10 examined in this study.

One reason to study the dependence of the CID pattern on different ion trap parameters is the wish to compare different PIT-MS systems and to make a database of CID patterns for compounds often observed. Since the proton-transfer reaction ionization is so versatile, the amount of compounds that could be observed is very large and characterization of the system for all possible compounds is a virtually endless task. We show that the fragmentation ratios are independent of the helium flow and the excitation q_z-value, when the fragments are expressed as fractions of the total ion intensities stored after dissociation. However, different internal ion energies could influence the fragment ratios when two or more dissociation pathways compete. Liere et al. [33] reported a clear influence of the ion internal energy on the fragmentation ratio of *n*-butylbenzene. They show that different internal energies of the *n*-butylbenzene ion favor either the low or high internal energy dissociation pathway, lead-

ing to different ratios for the products mass 91 or 92. A similar effect is observed in our case on α-terpinene.

Our results show that it is not straightforward to compare CID patterns from different/differently configured systems. A comparison between the CID patterns of different instruments and the dependence of the patterns on different parameters could elucidate this question.

The conventional, quadrupole mass filter-equipped PTR-MS instrument cannot distinguish different monoterpenes species. Therefore, usually the sum of the ion signals on mass 81 and 137 amu (or only mass 137 amu) is adopted as a measure for total monoterpenes [35,38,39]. We show here that it is possible to distinguish between several different compounds solely on the basis of their CID patterns, using our PIT-MS instrument. This shows that the CID method is a very useful addition to the PTR techniques.

Acknowledgements

The authors would like to thank Gerben Wulterkens and Edwin Sweers for their excellent technical assistance in, respectively, designing and building most parts of the PIT-MS instrument; all the people from Interscience BV, Breda, The Netherlands; Peter Claus for providing electronic solutions to all our practical problems and Joost de Gouw and Carsten Warneke (NOAA, Boulder, CO, USA) for our very useful discussions. The project was financially supported by the Dutch Foundation for Research on Matter (FOM).

References

[1] W. Lindinger, A. Hansel, A. Jordan, Int. J. Mass Spectrom. 173 (1998) 191.
[2] T. Karl, A. Guenther, Int. J. Mass Spectrom. 239 (2004) 77.
[3] C. Warneke, J. De Gouw, W. Kuster, P. Goldan, R. Fall, Environ. Sci. Technol. 37 (2003) 2494.
[4] J. de Gouw, C. Warneke, T. Karl, G. Eerdekens, C. van der Veen, R. Fall, Int. J. Mass Spectrom. 223–224 (2003) 365.
[5] A. Boschetti, F. Biasioli, M. van Opbergen, C. Warneke, A. Jordan, R. Holzinger, P. Prazeller, T. Karl, A. Hansel, W. Lindinger, S. Iannotta, Postharv. Biol. Technol. 17 (1999) 143.
[6] E. Boamfa, M. Steeghs, S. Cristescu, F. Harren, Int. J. Mass Spectrom. 239 (2004) 193.
[7] A. Critchley, T. Elliott, G. Harrison, C. Mayhew, J. Thompson, T. Worthington, Int. J. Mass Spectrom. 239 (2004) 235.
[8] P. Lirk, F. Bodrogi, J. Rieder, Int. J. Mass Spectrom. 239 (2004) 221.
[9] A. Jordan, A. Hansel, R. Holzinger, W. Lindinger, Int. J. Mass Spectrom. Ion Process. 148 (1995) L1.
[10] C. Warneke, J. Kuczynski, A. Hansel, A. Jordan, W. Vogel, W. Lindinger, Int. J. Mass Spectrom. Ion Process. 154 (1996) 61.
[11] M. Steeghs, H. Bais, J. de Gouw, P. Goldan, W. Kuster, M. Northway, R. Fall, J. Vivanco, Plant Physiol. 135 (2004) 47.
[12] T. Karl, A. Curtis, T. Rosenstiel, R. Monson, R. Fall, Plant Cell Environ. 25 (2002) 1121.
[13] R. Fall, T. Karl, A. Hansel, A. Jordan, W. Lindinger, J. Geophys. Res. Atmos. 104 (1999) 15963.
[14] D. Ezra, J. Jasper, T. Rogers, B. Knighton, E. Grimsrud, G. Strobel, Plant Sci. 166 (2004) 1471.
[15] K. Buhr, S. van Ruth, C. Delahunty, Int. J. Mass Spectrom. 221 (2002) 1.
[16] F. Gasperi, G. Gallerani, A. Boschetti, F. Biasioli, A. Monetti, E. Boscaini, A. Jordan, W. Lindinger, S. Iannotta, J. Sci. Food Agric. 81 (2001) 357.
[17] M. Mestres, N. Moran, A. Jordan, A. Buettner, J. Agric. Food Chem. 53 (2005) 403.
[18] R. Dorfner, T. Ferge, C. Yeretzian, A. Kettrup, R. Zimmermann, Anal. Chem. 76 (2004) 1386.
[19] C. Lindinger, P. Pollien, S. Ali, C. Yeretzian, I. Blank, T. Mark, Anal. Chem. 77 (2005) 4117.
[20] M.M.L. Steeghs, B.W.M. Moeskops, K. van Swam, S.M. Cristescu, P.T.J. Scheepers, F.J.M. Harren, Int. J. Mass Spectrom. 253 (2006) 58.
[21] C. Warneke, J.A. de Gouw, E.R. Lovejoy, P.C. Murphy, W.C. Kuster, J. Am. Soc. Mass Spectrom. 16 (2005) 1316.
[22] P. Prazeller, P. Palmer, E. Boscaini, T. Jobson, M. Alexander, Rap. Commun. Mass Spectrom. 17 (2003) 1593.
[23] C. Warneke, S. Kato, J.A. De Gouw, P.D. Goldan, W.C. Kuster, M. Shao, E.R. Lovejoy, R. Fall, F.C. Fehsenfeld, Environ. Sci. Technol. 39 (2005) 5390.
[24] T. Karl, F.J.M. Harren, C. Warneke, J.A. de Gouw, C. Grayless, R. Fall, J. Geophys. Res. Atmos. 110 (2005) D15.
[25] C. Warneke, S. Rosen, E. Lovejoy, J. de Gouw, R. Fall, Rap. Commun. Mass Spectrom. 18 (2004) 133.
[26] M.M.L. Steeghs, C. Sikkens, E. Crespo, S.M. Cristescu, F.J.M. Harren, Int. J. Mass Spectrom. 262 (2007) 16–24.
[27] T. Wang, P. Spanel, D. Smith, Int. J. Mass Spectrom. 239 (2004) 139.
[28] T.M. Ruuskanen, Bor. Environ. Res. 10 (2005) 553.
[29] S. Hayward, A. Tani, S. Owen, C. Hewitt, Tree Physiol. 24 (2004) 721.
[30] A. Tani, S. Hayward, C. Hewitta, Int. J. Mass Spectrom. 223 (2003) 561.
[31] A. Lee, G. Schade, R. Holzinger, A.H. Goldstein, Atm. Chem. Phys. 5 (2005) 505.
[32] C. Hao, R.E. March, Int. J. Mass Spectrom. 212 (2001) 337.
[33] P. Liere, R.E. March, T. Blasco, J.-C. Tabet, Int. J. Mass Spectrom. Ion Process. 153 (1996) 101.
[34] N. Schoon, C. Amelynck, L. Vereecken, E. Arijs, Int. J. Mass Spectrom. 229 (2003) 231.
[35] A. Wisthaler, N. Jensen, R. Winterhalter, W. Lindinger, J. Hjorth, Atm. Environ. 35 (2001) 6181.
[36] A. Tani, S. Hayward, A. Hansel, C. Hewitt, Int. J. Mass Spectrom. 239 (2004) 161.
[37] R.E. March, F.A. Londry, R.L. Alfred, A.M. Franklin, J.F.J. Todd, Int. J. Mass Spectrom. Ion Process. 112 (1992) 247.
[38] W. Grabmer, M. Graus, C. Lindinger, A. Wisthaler, B. Rappengluck, R. Steinbrecher, A. Hansel, Int. J. Mass Spectrom. 239 (2004) 111.
[39] R. Holzinger, A. Lee, M. McKay, A.H. Goldstein, Atm. Chem. Phys. 6 (2006) 1267.